

Original Paper

# Mast Cell Changes the Phenotype of Microglia via Histamine and ATP

María Pilar Ramírez-Ponce<sup>a</sup> Alejandro Sola-García<sup>a</sup> Santiago Balseiro-Gómez<sup>a,b</sup>  
María Dolores Maldonado<sup>c</sup> Jorge Acosta<sup>a</sup> Eva Alés<sup>a</sup> Juan Antonio Flores<sup>a,c</sup>

<sup>a</sup>Departamento de Fisiología Médica y Biofísica, Facultad de Medicina, Universidad de Sevilla, Sevilla, Spain, <sup>b</sup>Department of Neuroscience, Yale School of Medicine, New Haven, CT, USA, <sup>c</sup>Departamento de Bioquímica Médica y Biología Molecular e Inmunología, Facultad de Medicina, Universidad de Sevilla, Sevilla, Spain

## Key Words

Exocytosis • Phagocytosis • Histamine • ATP • Mast cells • Microglia

## Abstract

**Background/Aims:** Microglia are the dynamic motile phagocytes of the brain considered the first line of defense against threats or disturbances to the Central Nervous System (CNS). Microglia help orchestrate the immunological response by interacting with others immune cells. Mast cells (MCs) are effector cells of the innate immune system distributed in all organs and vascularized tissues, brain included. Several molecular mechanisms for potential interactions between MCs and microglia have been determined. However, the effect of MCs on regulated exocytosis and phagocytic clearance in microglia has not been explored. **Methods:** Cocktails of MCs mediators (MCM) obtained at 37°C and 53°C were used to induce microglia activation. Changes in intracellular calcium  $[Ca^{2+}]_i$  and ATP release were studied by calcium and quinacrine fluorescence imaging. Fluorescent latex beads were used to assay phagocytosis in microglia after MCM treatment and compared to that measured in the presence of histamine, ATP and lipopolysaccharide (LPS). Iba-1 expression and area were quantified by immunofluorescence and histamine levels evaluated by ELISA techniques. **Results:** Local application onto microglia of the MC mediator cocktail elicited  $Ca^{2+}$  transients and exocytotic release associated with quinacrine dye de-staining.  $Ca^{2+}$  signals were mimicked by histamine and blocked by the H1 receptor (H1R) antagonist, cetirizine. Hydrolysis of ATP by apyrase also affected  $Ca^{2+}$  transients to a lesser extent. Iba-1 fluorescence, cell area and phagocytosis were enhanced by histamine through H1R. However, ATP prevented iba-1 expression and microglial phagocytosis. MCM showed combined effects of histamine and ATP, increasing the number of internalized microbeads per cell and area without raising iba1 expression. **Conclusion:** Our results highlight the relevance of MC-derived histamine and ATP in the modulation of secretory and phagocytic activities that would explain the heterogeneity of microglial responses in different pathological contexts.

© 2021 The Author(s). Published by  
Cell Physiol Biochem Press GmbH&Co. KG

## Introduction

Chronic inflammation in CNS is a hallmark of neurodegenerative disorders in which progressive loss of neurons and altered physicochemical properties in the brain are observed [1, 2]. Microglia cells, key players in such disorders, are the resident macrophages of the brain and play an important role in maintaining normal brain function. Pathological states within the nervous system can lead to microglial activation, characterized by morphological changes, proliferation, and migration towards the injury site; phagocytosis; and secretion of various cytokines, chemokines, and other inflammatory mediators [3]. Activation of microglial cells can result in different phenotypes and roles (neurotoxic or neuroprotector) with versatile actions and variable responses depending on the stimulus intensity and context [4].

In their resting state, microglial cells display a ramified morphology characterized by numerous, fine-branched processes with relatively small bodies. When activated in response to injury or inflammatory stimuli, the resting microglia increase  $\text{Ca}^{2+}$  permeability that leads to  $\text{Ca}^{2+}$  influx into the cells. This increase of intracellular calcium  $[\text{Ca}^{2+}]_i$  acts as a versatile intracellular second messenger that initiates signaling cascades, leading to essential biological processes such as the morphological transformation [5] in which cells become progressively less ramified and quickly develop an ameboid appearance with an enlarged cell body and several short, thickened processes. Elevations of  $[\text{Ca}^{2+}]_i$  in microglial cells is also required in ATP and BDNF secretion through  $\text{Ca}^{2+}$  dependent exocytosis from lysosomes and secretory granules [6, 7]. Given the involvement of lysosomal secretion in cytokine release [8, 9], the exocytotic process can be crucial to define the phenotype acquired by these plastic cells upon activation. In addition, microglial functions such as motility and phagocytosis are closely associated with dynamic changes in the cytoskeleton and related to intracellular calcium signaling [10, 11].

Microglia can respond to pro-inflammatory signals released from other non-neuronal cells of immune origin, which include mast cells (MCs). These cells reside in the brain and can traverse the blood-brain barrier in healthy and pathological conditions [12, 13]. MCs contain numerous secretory granules that hold a wide spectrum of mediators, including biogenic amines such as histamine and serotonin, enzymes, ATP, neuropeptides and proteoglycans [14]. In addition to rapid mediator release of preformed granule constituents via degranulation, longer-term activation results in the release of the *novo* formed mediators such as lipid mediators and cytokines [15]. Brain MCs are activated in CNS disorders and induce the release of several mediators. MCs were reported to induce microglial activation and inflammatory mediator release [16, 17] suggesting a pivotal role of these cells in the induction of CNS inflammation. Thus, the suppression or stabilization of brain MCs degranulation can inhibit both microglial activation and CNS inflammation [18-20].

Mast cell-microglia communication contributes to accelerate disease progression. However, the functional consequences of MCs in microglial exocytosis and phagocytosis remain unexplored. Microglia activation is associated to secretion of several molecules, which either propagate inflammation and cause damage to neurons or play a neuroprotective role [21]. Microglia also phagocytizes foreign pathogens, apoptotic cells, myelin debris and released toxic proteins. In this study, we imaged changes in  $[\text{Ca}^{2+}]_i$  and, measured exocytosis of ATP-containing vesicles and the phagocytic activity of microglia evoked by a cocktail of MCs mediators. Our results suggest MC may trigger microglia activation that results in functional responses determined by the contribution mainly of histamine but also ATP.

## Materials and Methods

### *Cocktail of mast cells mediators*

A cocktail of mast cells mediators (Mast cells Conditioned Medium, MCM) was prepared as previously described [22]. Briefly,  $1 \times 10^6$  purified MCs obtained after a 70% Percoll purification were resuspended in 1 ml of basal Locke solution containing 140 mM NaCl, 10 mM HEPES, 3 mM KOH, 2 mM  $\text{CaCl}_2$ , 1 mM  $\text{MgCl}_2$ , and 10 mM glucose (pH 7.3, adjusted with NaOH). Cells were placed into a prewarmed Thermomixer (Eppendorf) for 1 h at 53°C with moderate agitation (600 rpm). MC degranulation was verified by visual inspection under a microscope. The MCM was obtained from the supernatant after centrifugation of MCs solution at 200xg for 5 min. Supernatant was aliquoted (50  $\mu\text{l}$ ) and stored at -80°C until use. MCM from MCs kept at 37°C, 5%  $\text{CO}_2$  for 1 h was obtained to evaluate the degree of degranulation in basal conditions.

### *Enzyme-Linked Immuno-Sorbent Assay (ELISA)*

The expression of histamine levels in MCM was quantified with a commercial ELISA kit from Beckman Coulter (IMMUNOTECH – Prague, Czech Republic) following the manufacturer's instructions. All samples were run in duplicate.

### *Microglia-Enriched Cultures*

Isolated microglia were obtained using a mild trypsinization over mixed glial cultures as previously described [23] with slight modifications.

Mixed glial cultures were prepared from cerebral cortices of postnatal (P2-P4) Wistar rats, which were subjected to mechanical dissociation. After filtering cells through a filter nylon mesh of 100  $\mu\text{m}$ , the cells obtained were seeded in Dulbecco's modified Eagle's medium (DMEM)/F12 with 20% of inactivated foetal bovine serum (FBS) at a density of 300,000 cells/ml on 15 mm-diameter cover glass and maintained at 37°C in a humidified atmosphere of 5%  $\text{CO}_2$ /95% air. Culture medium was replaced after 5 days *in vitro* (DMEM/F12 and 10% of inactivated FBS). After reaching a confluent monolayer of glial cells (10-12 days), microglia-enriched cultures were obtained with a trypsin solution (0,05% trypsin and EDTA) diluted 1:4 in DMEM/F12. This process resulted in the detachment of the upper layer of cells in one piece, while microglial cells remained attached on the surface of the cover glass. Mild trypsinization has been proved to be a reliable method to isolate microglia from mixed glial cultures with increased yield and purity, and microglial cells seem to be in an immune state closer to their resting state in comparison with the shaking method [24]. However, our cultures did not exceed 15% of cells with a resting phenotype.

### *Recordings of $[\text{Ca}^{2+}]_i$ signal*

Changes in  $[\text{Ca}^{2+}]_i$  of microglial cells in response to different stimuli were monitored by dual excitation microfluorimetry. Microglial cells were incubated in Locke external solution containing Fura-2 AM 5  $\mu\text{M}$  (Molecular Probes) and pluronic F-127 0.004%, (Sigma) for 45 min at 37°C in the dark. Later, cells were washed twice in external solution without the dye and used for imaging. The cover glass with cells loaded with Fura-2 AM was then mounted in a RC-25F perfusion chamber (Warner instruments) and placed on the microscope (AxioVert 200, Zeiss). During recordings, microglial cells were excited by a xenon light source at 360/380-nm wavelengths (exposure time, 0.5 s; data acquisition at 0.33 Hz) by means of two narrow band-pass filters selected by a computer-controlled wheel. The emitted fluorescence was filtered through a 520-nm filter and captured with an ORCA-R2 CCD camera (Hamamatsu Photonics). Fura-2 AM loading was usually uniform over the cytoplasm, and dye compartmentalization was never observed. Data were acquired and stored using HCLImage software and exported to Igor Pro (WaveMetrics) to perform analysis. All values were normalized to the basal fluorescence (baseline). The  $[\text{Ca}^{2+}]_i$  signal was expressed by the ratio of fluorescence at 360 nm and 380 nm. The agents used to stimulate microglia were MCM, histamine 100  $\mu\text{M}$ , serotonin 100  $\mu\text{M}$  and ATP 100  $\mu\text{M}$ . When required, cells were incubated with cetirizine 1  $\mu\text{M}$ , ranitidine 10  $\mu\text{M}$ , carbinine 10  $\mu\text{M}$  or A943931 10  $\mu\text{M}$ , antagonists of H1R, H2R, H3R and H4R, respectively, or FSLRLY-NH2 (PAR2 antagonist) 400  $\mu\text{M}$  for 10 min at 37°C before the application of MCM or histamine. MCM was treated with apyrase 50 U/ml for 10 min, chondroitinase ABC 50 mU/ml or heparinase 0.5 U/ml for 1 h at 37°C to evaluate the effect of ATP, chondroitin sulphate or heparin from the MCM on microglial cells, respectively. These products were applied through a pressure pulse (5 s) with a micropipette (1  $\mu\text{m}$  diameter) positioned approximately 100  $\mu\text{m}$  to the microglial cell. All experiments were performed at 37°C.

### *Imaging and analysis of Quinacrine dye release*

To visualize microglial acidic organelles, microglia was treated with 10  $\mu\text{M}$  quinacrine in Locke external solution for 10 min at 37°C in the dark. Later, microglial cells were washed twice in external solution without the dye and used for imaging. The cover glass with cells loaded with quinacrine was then mounted and transfer to the chamber for imaging under an inverted microscope with a 63 $\times$  PlanNeofluar (NA 1.3) oil immersion lens (Zeiss). The fluorescence images were collected every 5s, with excitation at 472 nm and emission at 579 nm. Data analysis was performed with HCLImage software (Hamamatsu). Time-lapse imaging of quinacrine fluorescence was evaluated after application of MCM, histamine 100  $\mu\text{M}$ , ATP 100  $\mu\text{M}$  and LPS 1  $\mu\text{g}/\text{ml}$ .

### *Phagocytosis Assay and Microglia Immunofluorescence*

After mixed glia culture was subjected to trypsin treatment, microglial cells were allowed to recover for 24h, after which the cells were ready to undergo some microglial treatments for 48h. These treatments were as follows: control (without any treatment), MCM, 1 $\mu\text{g}/\text{ml}$  of LPS, 4  $\mu\text{M}$  histamine, 100  $\mu\text{M}$  histamine, 10  $\mu\text{M}$  ATP and 100  $\mu\text{M}$  ATP. When required, cells were incubated with cetirizine 1  $\mu\text{M}$ , ranitidine 10  $\mu\text{M}$ , carcinine 10  $\mu\text{M}$  or A943931 10  $\mu\text{M}$ . Later, we proceeded to the phagocytosis assay (blind experiments). This is as follows (with some modifications [25]). Fluorescent latex beads were used to assay phagocytosis. Fluorescent beads were pre-opsonized in non-inactivated FBS for 1h at 37°C. Ratio of beads to FBS was 1:5. Beads-containing FBS with DMEM/F12 with 10% of inactivated FBS were diluted to reach final concentrations for beads and FBS in DMEM/F12 of 0.01% (v/v) and 0.05% (v/v), respectively. Then, cell cultures were incubated with beads-containing medium at 37°C for 1h and washed thoroughly with ice-cold PBS 5 times. Next, cells were fixed using 4% PFA for 30 min at room temperature. After that, we performed iba-1 immunofluorescence. Firstly, cells were permeabilized with 0.1% Triton X-100 in PBS and, after adding blocking solutions for 1h at room temperature, incubated overnight with rabbit anti-iba1 monoclonal antibody (1:1000) (Synaptic Systems) at 4°C. Cells were washed five times with PBS, then incubated with Alexa Fluor 555-conjugated goat anti-rabbit secondary antibody (1:500) (Molecular Probes) at room temperature for 1h. After this, cells were washed five times with PBS and mounted on cover glasses with Fluoromont-G medium. Fluorescent images were randomly acquired using an inverted microscope (AxioVert 200, Zeiss). To visualize the iba-1 staining, microglia were excited by a xenon light source at 552 nm wavelength (exposure time, 0.8 s); in the case of beads, these were excited with a FITC-filter at 495 nm (exposure time, 0.08 s). The emission wavelengths were 578 and 519 nm, respectively. For the study of the effects of MCM and the rest of treatments on the number of phagocytosed beads (mean  $\pm$  S.E.M.), bead-labelled cells were counted in four separate culturing procedures under the microscope with a 40x objective (blind analysis). Microglial cell area and intensity were measured from iba-1 cell fluorescence images through automatic thresholding selection (HCLImage).

### *Statistical Analysis*

Statistical analyses were carried out with the Mann-Whitney Rank Sum test or the Student's t test (SPSS Statistics 25). All measurements were expressed as mean  $\pm$  standard error of the mean (SEM), and  $p \leq 0.05$  was considered significant.

## Results

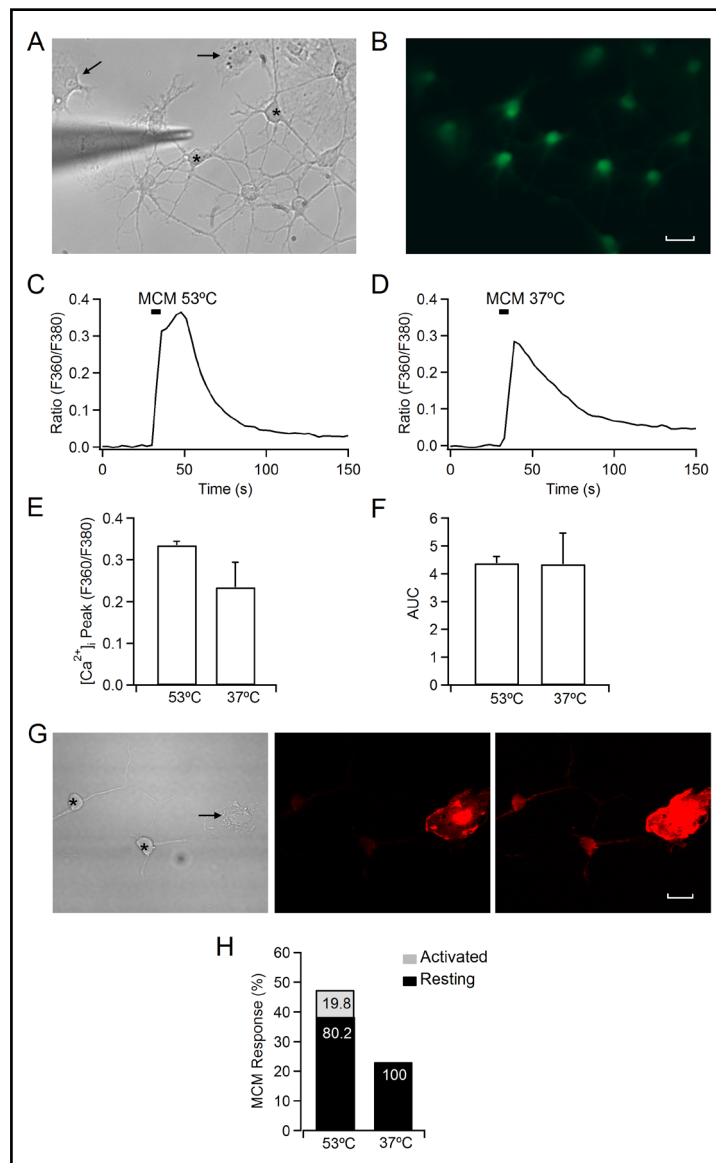
### *MCM triggers calcium transients essentially in resting microglia*

In the present study, we stimulated cultured rat microglial cells with a pressure pulse (5 s) of MCM (Fig. 1A). This cocktail of MCs mediators obtained by heat (53°C, 1 h), showed a rapid and transient elevation of intracellular calcium ( $[\text{Ca}^{2+}]_i$ ) in one out of two cells (167 out of 353 cells) measured by Fura-2 fluorescence (Fig. 1B, C). As MCs are temperature sensitive, the noxious physical stimuli (53°C) produced a clear degranulation verified by visual inspection under microscope (Supplementary Fig. 1B – for all supplementary material see [www.cellphysiolbiochem.com](http://www.cellphysiolbiochem.com)). This strategy elicits MC degranulation and avoids the use of stimuli such as compound 48/80, antigens, complement proteins or neuropeptides which can also activate microglia themselves. Interestingly, MCM obtained at 37°C, was

also able to trigger intracellular  $\text{Ca}^{2+}$  elevation in 27% (6 out of 22) of microglial cells. At this temperature, MCs showed an intact appearance without clear degranulation (Fig. 1A Supplementary). The increase in intracellular  $\text{Ca}^{2+}$  evoked in microglial cells by MCM at  $37^\circ\text{C}$  was also transient and reached a peak of  $0.23 \pm 0.06$  and area under curve (AUC) of  $4.34 \pm 1.12$  that were similar to that induced by the MCM obtained by heat ( $53^\circ\text{C}$ ) ( $\Delta\text{F}/\text{F}$ :  $0.33 \pm 0.01$ ; AUC:  $4.38 \pm 0.24$ ) (Fig. 1E, F).

Microglial cells with a ramified morphology with long, thin processes and small cell bodies are the major responders to the MCM (80.2 % at  $53^\circ\text{C}$  and 100% at  $37^\circ\text{C}$ ) (Fig. 1G, H). These cells exhibit shapes typical of resting microglia and a weaker *iba1* signal, a microglia-specific calcium-binding protein, in comparison with expression of *iba1* in spindle, rod or amoeboid-shaped cells, corresponding to activated microglia (Fig. 1G). These data suggest that low secretion of mediators, such as the escape of biogenic amines from granules during basal activity of MCs ( $37^\circ\text{C}$ ) is sufficient to evoke  $\text{Ca}^{2+}$  elevations mainly in those microglial cells with a resting phenotype. All the experiments carried out below were performed with a MCM obtained after degranulation of MCs at  $53^\circ\text{C}$  to make sure full release of granule mediators.

**Fig. 1.** Calcium imaging of microglial cells. A) Phase-contrast image of rat cultured microglia and a glass micropipette of  $1\mu\text{m}$   $\phi$  connected to a picospritzer which applies 5 s pressure ejection (2.5 psi) pulses. B) Fluorescence image showing the same cells loaded with the  $\text{Ca}^{2+}$  sensitive dye Fura 2-AM. C) Representative trace of  $[\text{Ca}^{2+}]_i$  transient in a cell evoked by the application of MCM obtained after MCs degranulation at  $53^\circ\text{C}$ . D) Representative trace of  $[\text{Ca}^{2+}]_i$  transient in a cell evoked by application of MCM obtained after MCs incubation at  $37^\circ\text{C}$ . E) Mean  $[\text{Ca}^{2+}]_i$  peak and F) Area under curve (AUC) obtained in microglia-evoked responses by stimulation with MCM at  $53^\circ\text{C}$  and  $37^\circ\text{C}$ . G) Anti-*Iba1* immunostaining of microglial cells with different morphological phenotype (2 resting cells with ramified long processes and rounded cell bodies (\*) and 1 activated cell with an amoeboid appearance (arrow)). Left panel shows cells in bright-field, middle and right panels show fluorescence images taken at 60X and a 366 hV and 536 hV of gain, respectively. H) Percentage of microglia activated by MCM at  $53^\circ\text{C}$  and  $37^\circ\text{C}$ . Numbers inside the bars indicate the proportion of activated or resting cells that showed a  $[\text{Ca}^{2+}]_i$  transient after MCM application. Scale bar:  $10\mu\text{m}$ .



*Histamine and ATP are the mediators involved in microglia evoked Ca<sup>2+</sup> transient*

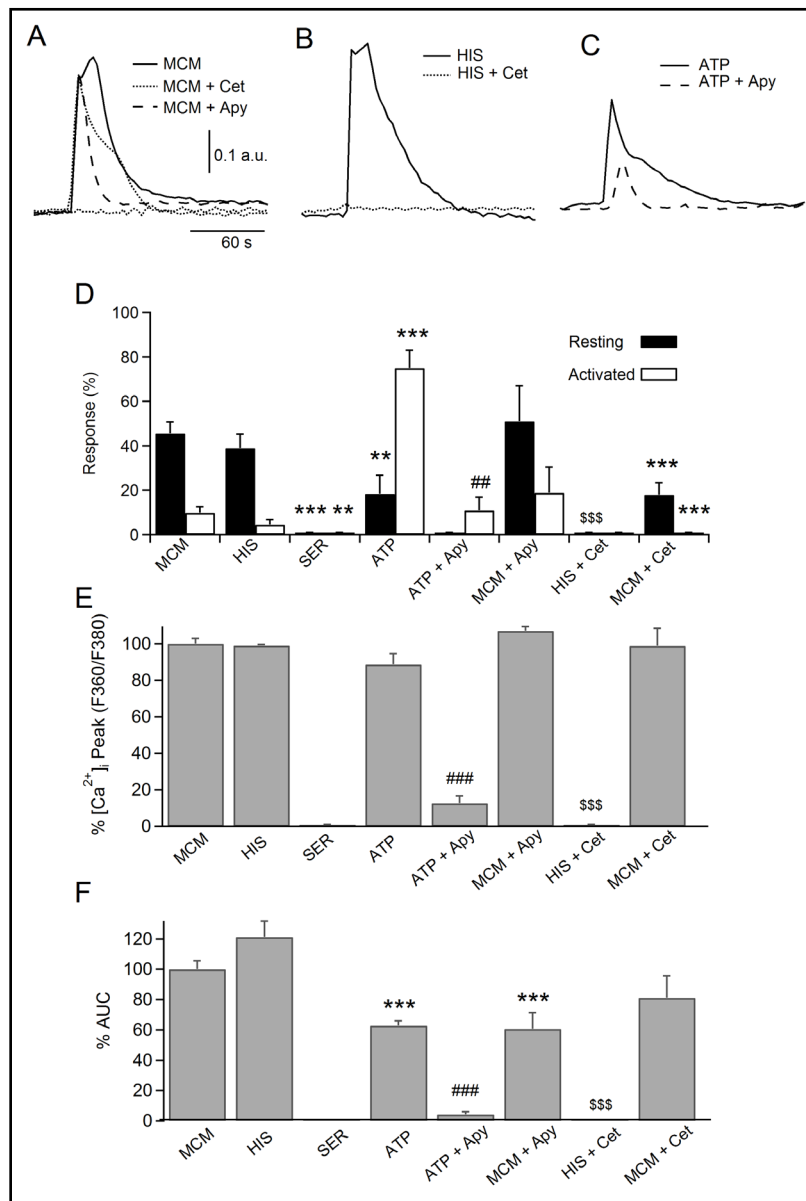
We investigated which mediators were involved in this Ca<sup>2+</sup> signaling. MCs contain a wide array of chemical mediators that can be released to the extracellular medium. We focused on the preformed products contained within the granules. To elucidate which mediators were involved in the promotion of microglia activation, we first directly stimulated microglial cells with bioactive monoamines (histamine, serotonin) and ATP. The effects of histamine (100 μM) on Ca<sup>2+</sup> signal in microglial cells were similar to those elicited by MCM at 53°C (Fig. 2A, B), with a 43% of response (83 out of 192 cells) (Fig. 2D) and, a [Ca<sup>2+</sup>]<sub>i</sub> peak and area under curve of 99.1 ± 0.6% and 121.2 ± 10.5 %, respectively (Fig. 2E, F). Histamine mostly affected intracellular Ca<sup>2+</sup> of resting cells (81.9% of responding cells) in consonance with the effects observed with MCM (80.2% of cells). However, serotonin did not evoke any response. On the contrary, external application of ATP (100 μM) caused a Ca<sup>2+</sup> transient (Fig. 2C) in most of the stimulated cells (94.8 %; 128 out of 135 cells) basically in activated microglia (70.9%) (Fig. 2D). In addition, while [Ca<sup>2+</sup>]<sub>i</sub> peak was not different (88.6 ± 6 %) (Fig. 2E), the area under the curve was significantly lower (62.8 ± 3.1 %) (Fig. 2F) in ATP than in MCM-stimulated cells. When the selective antagonist of the histamine H1 receptor, cetirizine, was incubated within the cell chamber, 10 min before the application of histamine, Ca<sup>2+</sup> transient response was completely abolished (Fig. 2B, D). However, neither ranitidine 10 μM (H2R antagonist), carbinine 10 μM (H3R antagonist) nor A943931 10 μM (H4R antagonist) modified [Ca<sup>2+</sup>]<sub>i</sub> peak and area under the curve induced by histamine 100 μM (Supplementary Table 1). Cetirizine also suppressed microglial activation induced by MCM, although a small pool of cells was resistant to the drug (10.3%; 21 out of 203 cells) (Fig. 2A, D). On the other hand, apyrase, an enzyme that catalyzes ATP hydrolysis, dramatically reduced ATP-response to 15.7 % (8 out of 51 cells); however, it did not affect MCM-microglia response (69.8%; 43 out of 61 cells) (Fig. 2A, C, D). Moreover, while [Ca<sup>2+</sup>]<sub>i</sub> peak and the area under the curve were abruptly reduced in cells under ATP + Apyrase (ΔF/F: 12.5 ± 4.1%; AUC: 4.3 ± 1.7%), the effect of apyrase on microglia response mediated by MCM was smaller; [Ca<sup>2+</sup>]<sub>i</sub> peak was similar (107 ± 2.4 %), however, the area under the curve was lower (60.6 ± 10.7 %) than that obtained by application of MCM alone (Fig. 2E, F).

Next, we selectively blocked PAR2 receptors with the antagonist FSLRY-NH2 to determine the involvement of mast cell-specific proteases. We incubated cells for at least 10 min with FSLRY-NH2 (400 μM) before proceeding to apply MCM. The drug barely modified [Ca<sup>2+</sup>]<sub>i</sub> signal evoked by MCM (ΔF: 107.5 ± 10.2%; AUC: 105.7 ± 8.6%; 38 out of 70 cells) (Fig. 3B, E, F). Lastly, to resolve the implication of highly anionic serglycin proteoglycans (PGs) containing glycosaminoglycan side chains of either heparin or chondroitin sulfate (CS) type in microglia activation, we incubated the MCM with heparinase or chondroitinase ABC for 1h at 37°C to break down the PGs of heparin and CS, respectively. Chondroitinase ABC did not change the peak amplitude and the area under the curve of [Ca<sup>2+</sup>]<sub>i</sub> transients in respect to untreated MCM (ΔF: 95.6 ± 9.25%; area under curve: 99.9 ± 9.1%; 16 out of 30 cells) (Fig. 3C,E,F). Similarly, heparinase neither reduced the amount of [Ca<sup>2+</sup>]<sub>i</sub> entry into the cell (ΔF: 78.5 ± 7.7%; area under curve: 106 ± 9.1%; 32 out of 55 cells) (Fig. 3D, E, F). All these data suggest histamine H1 receptor mostly contributes to intracellular Ca<sup>2+</sup> elevation in cultured microglia mediated by MCs. To a lesser extent, ATP also contributes in shaping the Ca<sup>2+</sup> transient. Because histamine is the key mediator to initiate Ca<sup>2+</sup> signaling that triggers microglia activation, we measured histamine concentration of used cocktails. On average, histamine concentration from MCM obtained at 53°C (1 h) was 275 ± 90 μM and at 37°C (1h) of 17.5 ± 0.6 μM.

*Ca<sup>2+</sup> dependent exocytosis in microglia stimulated by MCM and histamine*

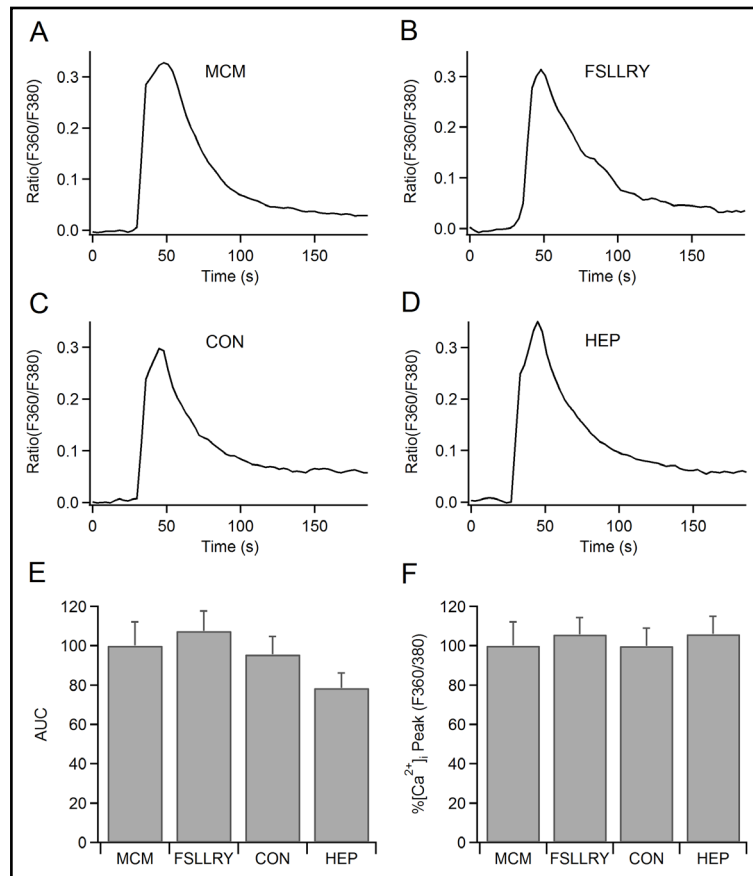
ATP is considered the major chemokine attracting microglia towards the injured brain regions [26] and microglia release ATP in response to stimuli which trigger intracellular calcium elevation [27]. Here, we incubated cells with quinacrine (10 μM for 10 min at room temperature), a fluorescent marker for intracellular ATP-enriched vesicles used to examine Ca<sup>2+</sup> dependent regulated exocytosis of ATP [6, 7]. We quantified exocytosis measuring

**Fig. 2.** Histamine and ATP contribute to outline the  $[Ca^{2+}]_i$  signal elicited by MCs mediator cocktail. A)  $[Ca^{2+}]_i$  signals evoked by single 5 s pressure ejection pulses of MCM alone (solid trace) and MCM applied after cetirizine (Cet) 1  $\mu$ M (dotted line) and apyrase (Apy) 50 U/ml (dashed line) treatment (10 min). B) Representative  $[Ca^{2+}]_i$  signals evoked by histamine (HIS) 100  $\mu$ M (solid line) and histamine 100  $\mu$ M applied after cetirizine 1  $\mu$ M (dotted line) treatment (10 min). C) Representative  $[Ca^{2+}]_i$  signals evoked by single pressure pulses of ATP 100  $\mu$ M (solid line) and ATP 100  $\mu$ M applied after apyrase 50 U/ml treatment (10 min) (dashed line). D) Percentage of stimulated cells which displayed  $[Ca^{2+}]_i$  transients in response to the different treatments according to the observed phenotype (resting vs activated). E)  $[Ca^{2+}]_i$  signal amplitude (peak) and F) area under curve (AUC) obtained by application of MCM, histamine 100, histamine following incubation with cetirizine (HIS + Cet), serotonin (SER), ATP, ATP after incubation with apyrase (ATP + Apy), MCM after incubation with cetirizine (MCM + Cet) and MCM after incubation with apyrase (MCM + Apy) are presented as % of means  $\pm$  SEM. Data were normalized regarding the MCM response. Statistically significant from MCM-treated cells (\*\* $p$ <0.001, \*\* $p$ <0.01). Statistically significant from ATP-treated cells (### $p$ <0.001, ## $p$ <0.01). Statistically significant from histamine-treated cells (\$\$\$ $p$ <0.001), using Mann-Whitney Rank Sum test.



fluorescence changes of cells after stimulation with MCM for 30s through a micro-perfusion pipette. As a control, application of an external solution produced a variable but gradual loss of fluorescence signal in 65% of cells which can be attributed to spontaneous vesicle fusion with the plasma membrane and dispersal of its fluorescent cargo (Fig. 4A, B, E). However, application of MCM induced a more abrupt loss of fluorescence (Fig. 4C, D, F) in 90.3% of cells to a significantly larger extent ( $\Delta F$ :  $0.43 \pm 0.02$ ;  $n=113$ ) than that observed in control cells ( $\Delta F$ :  $0.26 \pm 0.04$ ;  $n=40$ ). Furthermore, stimulation with histamine 100  $\mu$ M and LPS 1  $\mu$ g/ml also induced an important loss of fluorescence of  $0.5 \pm 0.04$  and  $0.49 \pm 0.02$ , respectively,

**Fig. 3.** PGs of CS and heparin, and proteases did not contribute to outline the  $[Ca^{2+}]_i$  signal elicited by mast cells mediator cocktail. A) Trace illustrating a control MCM-evoked response. B) The response did not change after incubation with FSLLRV-NH2. C) Neither pre-digestion of MCM with chondroitinase ABC nor D) heparinase modified  $[Ca^{2+}]_i$  transients. E)  $[Ca^{2+}]_i$  signal amplitude (peak) and F) area under curve (AUC) are presented as % of means  $\pm$  SEM.



in more than 92% of cells (Fig. 4H). ATP did not increase significantly the exocytosis in 89.5% of cells affected by the nucleotide. Cells with an activated morphology prevail over those of resting phenotype when measuring exocytosis in all used treatments (Fig. 4G). These results suggest that despite few activated microglia were able to rise  $[Ca^{2+}]_i$  in response to MCM, the vast majority of them undergo exocytosis of quinacrine loaded-organelles, comparable to that observed by histamine or LPS.

#### *Microglia metamorphosis induced by the MCM*

As microglial activation is characterized by morphological changes and upregulation of the specific calcium-binding protein iba1, we analyzed the area and iba1-fluorescence in cells iba1-positive from control cells and cells treated during 48 h with MCM, histamine 4 and 100  $\mu$ M, ATP 10  $\mu$ M and 100  $\mu$ M, and LPS 1  $\mu$ g/ml. Histamine concentration of used MCM was 3.7  $\mu$ M, obtained by dilution of the pure extract. For comparative purposes, we treated cells with histamine 4  $\mu$ M in addition to histamine 100  $\mu$ M. MCM showed a large increase in area ( $253.4 \pm 12 \mu\text{m}^2$ , n=372) in respect to control cells ( $154.9 \pm 5 \mu\text{m}^2$ , n=1117) (Fig. 5A, B) Histamine 4  $\mu$ M (HIS 4) and 100  $\mu$ M (HIS 100) also showed an increase in area ( $170.1 \pm 8 \mu\text{m}^2$ , n=605 and  $175.4 \pm 7 \mu\text{m}^2$ , n=354, respectively) although lower to that observed by MCM. LPS did not show an increment of area ( $155 \pm 9 \mu\text{m}^2$ , n=215) in respect to control cells. Finally, ATP 10  $\mu$ M showed an increase of area ( $200.8 \pm 6 \mu\text{m}^2$ , n=355) in respect to control cells as well as ATP 100  $\mu$ M ( $216.1 \pm 8 \mu\text{m}^2$ , n=495) (Fig. 5A, B). On the other hand, the effect of the cocktail of mediators did not change iba1 intensity ( $61.8 \pm 1.5$ ) in respect to control cells ( $62.5 \pm 1.5$ ) (Fig. 5C) but both histamine concentrations increased iba-1 expression (HIS 4:  $70.8 \pm 1.6$ ; HIS 100:  $69.6 \pm 1.4$ ). The higher increment was obtained with LPS ( $82.6 \pm 3.5$ ). ATP reduced iba1 intensity at 10  $\mu$ M ( $56.8 \pm 1.4$ ) and 100  $\mu$ M ( $53.8 \pm 1.5$ ). Overall, results on area and iba-1 expression by MCM on microglia may be the consequence of the summatory

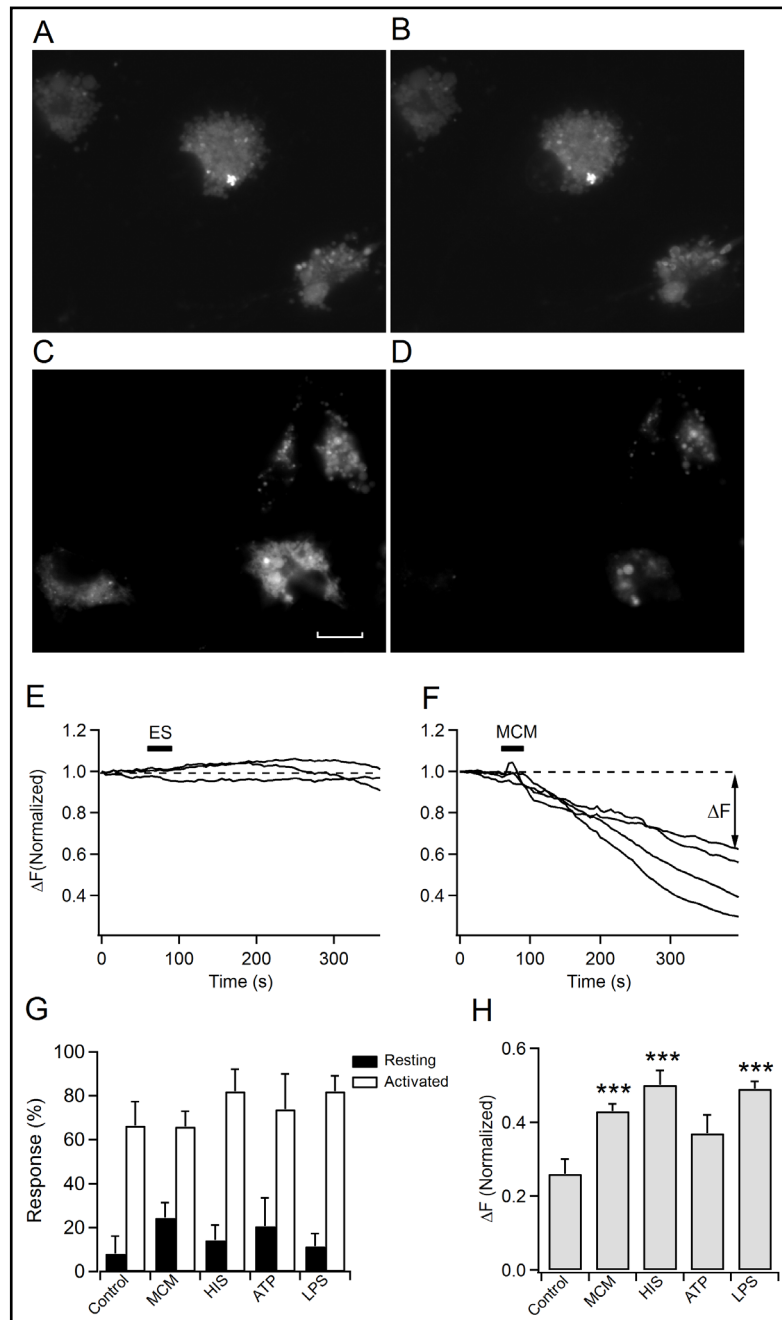


effects induced by ATP and histamine present in the MCM. MCM showed a potentiation of the area enlargement observed by histamine and ATP. Changes of iba-1 expression in the presence of ATP and histamine are similar but in the opposite sign, therefore the outcome of both combined mediators in the MCM may be the absence of modification in this parameter.

*The phagocytotic phenotype of microglia is determined by histamine*

Phagocytosis was assessed by using fluorescent latex beads of 1  $\mu\text{m}$  diameter under the same conditions and incubation intervals as above. MCM ( $\approx 4 \mu\text{M}$  histamine), histamine 4  $\mu\text{M}$  and 100  $\mu\text{M}$  showed an increase in the engulfment of microspheres per cell (MCM:  $2.91 \pm 0.3$ ,  $n=393$ ; HIS 4:  $2.71 \pm 0.24$ ,  $n=639$ ; HIS 100:  $3.08 \pm 0.27$ ,  $n=544$ ) regarding control cells ( $2.08 \pm 0.13$ ,  $n=1291$ ) (Fig. 6A, B). Histamine 20  $\mu\text{M}$  was also used ( $2.98 \pm 0.31$ ) and it did not show

**Fig. 4.** Changes in fluorescence intensity of quinacrine-loaded cells during exocytosis. A) Example image of quinacrine loaded microglia cells before and B)  $\sim 5$  min after application of external solution by micro-perfusion (control experiment). C) Example image of quinacrine loaded microglia cells before and D)  $\sim 5$  min after application of MCM. A larger loss of fluorescence was observed in respect to control. E) Time courses of fluorescence changes (normalized) in control cells and F) MCM treated cells from the upper images. G) Percentage of microglial cells (resting versus activated) that showed a positive exocytotic response (fluorescence decay  $>5\%$   $F_{\text{INITIAL}}$ ) following stimulation with MCM, histamine (HIS), ATP, and LPS. H) Amplitude ( $\Delta F$ ) measured from fluorescence curves ( $F_{\text{INITIAL}} - F_{\text{FINAL}}$ ). Data represent average values of at least three independent culturing experiments.  $***p < 0.001$ , using the Mann-Whitney Rank Sum test. Scale bar 5  $\mu\text{m}$ .



significant differences respect to histamine 4 and 100  $\mu\text{M}$ , and to the same extent as LPS ( $2.91 \pm 0.25$ ,  $n=215$ ). ATP 10  $\mu\text{M}$  and 100  $\mu\text{M}$  did not modify significantly phagocytosis although there were a downward trend (ATP 10:  $2.01 \pm 0.21$ ,  $n=363$ ; ATP 100:  $1.87 \pm 0.14$ ,  $n=505$ ).

In order to understand how morphological changes and iba1-intensity can influence functional responses of microglia, we have related these two parameters with phagocytosed beads per cell. Interestingly, we observed a linear relationship between iba1 expression and engulfed beads (Fig. 6C). Higher fluorescence intensity indicates higher intakes of beads. MCM showed a higher number of internalized beads per cell that it would be expected by its observed iba-1 intensity. This is likely due to the opposite and combined effects of ATP and histamine on these two parameters. In contrast, there was no relation between area and the number of beads per cell in each condition (Fig. 6D).

Last, we determined the contribution of histamine receptors expressed in microglia on the phagocytosis mediated by histamine and MCM (Fig. 6E, F). Ceterizine 1  $\mu\text{M}$  inhibited the increment of phagocytosis mediated by histamine 100  $\mu\text{M}$  and MCM. However, ranitidine 10  $\mu\text{M}$ , carbinine 10  $\mu\text{M}$  and A943931 10  $\mu\text{M}$  did not show any effect. These data suggest that phagocytosis induced by histamine and MCM is mediated by H1R. Besides, histamine induced a morphological transformation during microglia activation. Cells with ramified phenotype changed to an ameboid form. This cellular metamorphosis was also mediated by H1R (Supplementary Fig. 2).

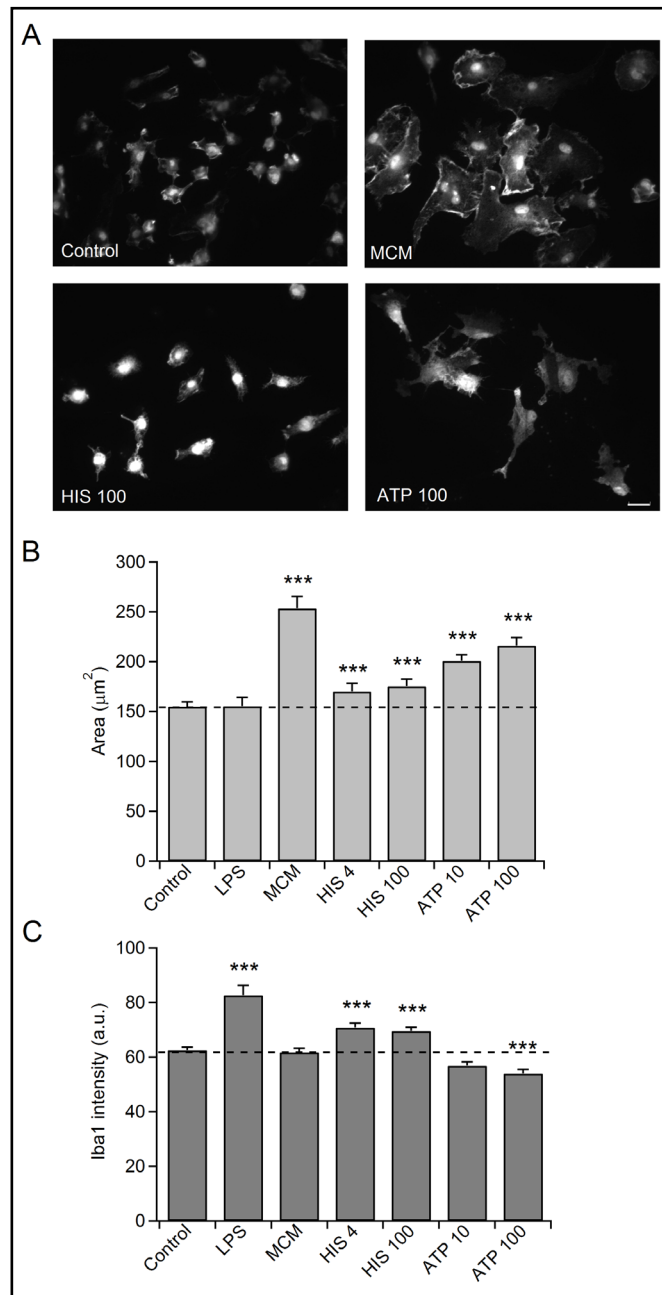


**Fig. 5.** MCM increases area but does not modify iba-1 expression in microglia. A) Representative images of iba1-positive microglia cells in non-treated cells (control), cells treated with MCM (MCM), histamine 100  $\mu\text{M}$  (HIS 100) and ATP 100  $\mu\text{M}$  (ATP 100). B) Surface area of cells treated for 48 h with MCM, histamine 4  $\mu\text{M}$  (HIS 4), histamine 100  $\mu\text{M}$  (HIS 100), ATP 10  $\mu\text{M}$  (ATP 10), ATP 100  $\mu\text{M}$  (ATP 100) and LPS 1  $\mu\text{g}/\text{ml}$  (LPS). C) Iba1 fluorescence intensity in cells treated for 48 h with MCM, HIS 4, HIS 100, ATP 10 and LPS. Values (mean  $\pm$  S.E.M) were computed from four independent culturing experiments. \*\*\* $p < 0.001$ , using the Mann-Whitney Rank Sum test. Scale bar 10  $\mu\text{m}$ .

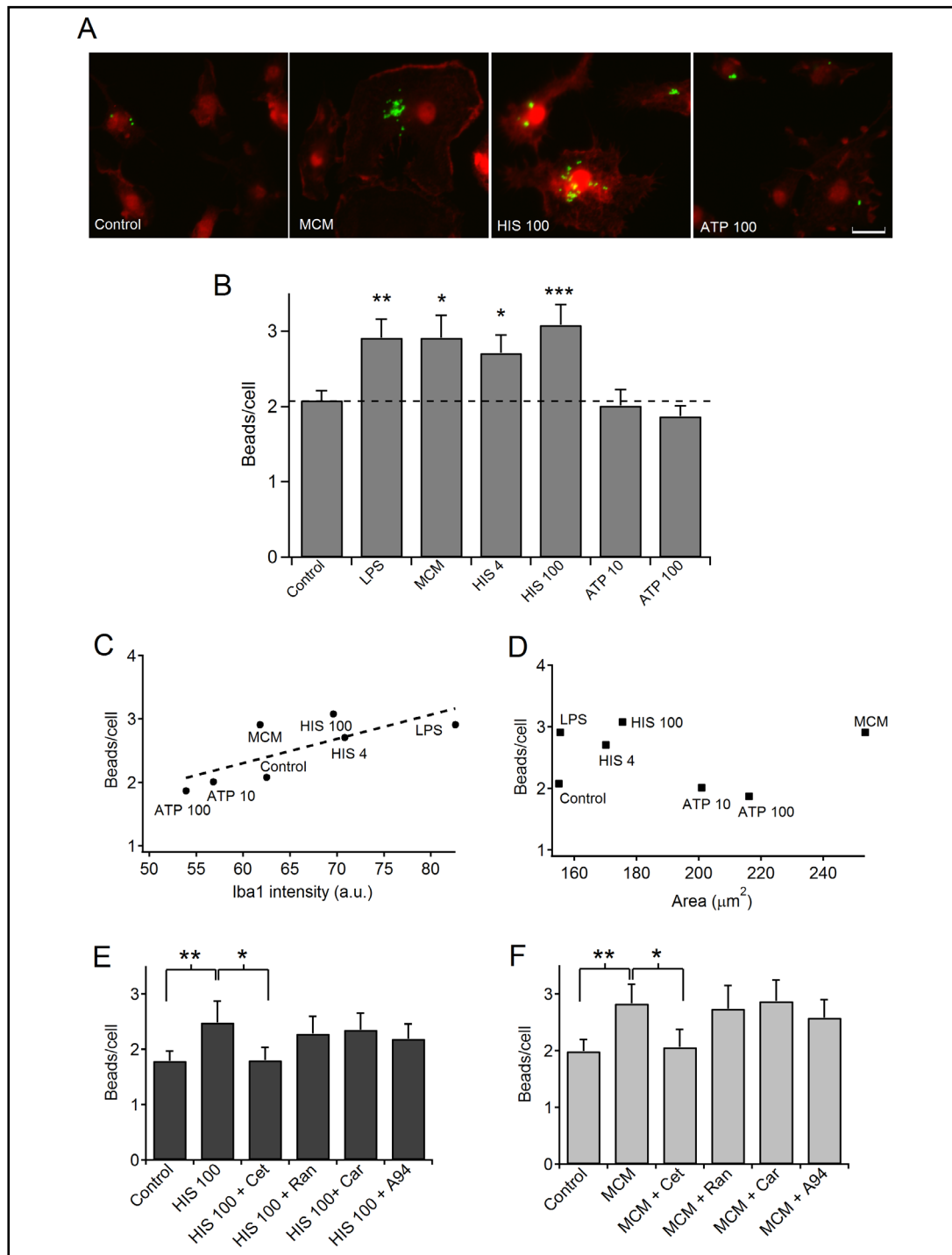


**Fig. 6.** MCM induces microglia phagocytosis via H1 receptor. A) Representative images illustrate latex microbeads phagocytosis of iba1-positive (red) microglial cells in non-treated cells (Control) and treated cells with, MCM, histamine 100  $\mu\text{M}$  (HIS 100) and ATP 100  $\mu\text{M}$  (ATP 100). B) Potentiation of phagocytosis by LPS, MCM, HIS 4 and HIS 100 at 48 h. No effect is induced by ATP 10 and ATP 100. C) Linear relation between iba1 intensity and beads per cell. D) Relationship between area and beads per cell. E) Phagocytosis induced by histamine 100  $\mu\text{M}$  (HIS 100) is inhibited by cetirizine (H1R antagonist) but not by ranitidine (H2R antagonist), carbinine (H3R antagonist) or A943931 (H4R antagonist). F) Phagocytosis induced by MCM is inhibited by cetirizine but not by ranitidine, carbinine or A943931, similarly to histamine. Values (mean  $\pm$  S.E.M) were computed from three independent culturing experiments. \* $p < 0.05$ ; \*\* $p < 0.01$ ; \*\*\* $p < 0.001$ , using the Student's t test. Scale bar 10  $\mu\text{m}$ .

## Discussion

In this work, we present data that suggest how MCs may activate microglia by causing an increase of intracellular  $[Ca^{2+}]_i$ . In basal conditions, MCs can undergo spontaneous exocytosis that results in secretion of histamine. Extracellular medium from resting MCs ( $10^6/ml$ ) kept for 1h at  $37^\circ C$  showed a histamine concentration of  $17 \mu M$ , a dose high enough to increase  $[Ca^{2+}]_i$  in only ramified (resting) microglia (Fig. 1D). At  $53^\circ C$ , MCs showed a degranulated phenotype, suggesting a stronger and complete degranulation able to increase histamine concentration to  $\approx 275 \mu M$  (on average). Curiously, in terms of  $Ca^{2+}$  signal, there were no differences in  $Ca^{2+}$  peak and the area under the curve of microglial cells activated by MCM at  $37^\circ C$  or  $53^\circ C$ , although a higher number of cells were affected at  $53^\circ C$ , which  $\approx 20\%$  of them were activated microglia (Fig. 1E, F, H). This activation in microglia is principally mediated by H1 receptor (H1R) since, after the blockade of H1R by cetirizine, the  $Ca^{2+}$  signal evoked by histamine  $100 \mu M$  was completely inhibited. To a much lesser extent, ATP seems to contribute to create the  $Ca^{2+}$  signal (Fig. 2C, F).

As ATP-exocytosis is triggered by an elevation of  $[Ca^{2+}]_i$ , we characterized  $Ca^{2+}$  dependent exocytosis in microglia by loading the cells with quinacrine. Although the increase in  $[Ca^{2+}]_i$  induced by MCM was mainly observed in resting microglia, we found a loss of quinacrine fluorescence mostly in activated cells. Microglia isolated from mixed cultures by mild trypsinization, as we performed, it is considered to show uniform ramified morphology unlike the more heterogeneous microglia isolated by using the shaking method [24]. Nevertheless, our cultures showed a certain level of activation and this activation at baseline may likely increase basal  $[Ca^{2+}]_i$  and affect the exocytotic response in stimulated and non-stimulated cells. Anyway, in response to MCM and histamine, microglia exhibited a higher exocytotic response than the one measured in control cells. Since lysosomal exocytosis has been suggested to be involved in cytokine release in monocytes and microglia [8, 9], it is likely that microglial exocytosis is at least partly responsible for the release of pro-inflammatory factors, such as tumor necrosis factor (TNF)-alpha and interleukine-6 (IL-6) from microglia stimulated with MC mediators [17]. Histamine, is a MC mediator which can stimulate microglia to activate in a dose-dependent manner and subsequently, generate the production of TNF- $\alpha$  and IL-6 [28]. The release of such mediators has been shown to be suppressed by H1R and H4R antagonists [17, 28]. This insight may partly confirm the abolishment of  $[Ca^{2+}]_i$  signal by the H1R antagonist cetirizine and suggests that TNF- $\alpha$  and IL-6 may be released by a  $Ca^{2+}$  dependent exocytosis.

Iba1 is a calcium-binding protein which is expressed specifically in microglia [29] and is upregulated in activated cells [30]. This is a cytoplasmic helix-loop-helix protein with F-actin binding and actin-cross-linking activity, possibly involved in cell motility and phagocytosis [30-32]. Our experiments confirm the role of iba1 in phagocytosis of longer activated microglia, given the relationship between iba1 intensity and phagocytosed microbeads (Fig. 6C). While LPS, histamine  $4$  and  $100 \mu M$  increased iba1 fluorescence and engulfed beads, ATP  $10$  and  $100 \mu M$  had the opposite effect, reducing iba1 signal and concomitantly, the phagocytic activity (Fig. 6C). MCM did not show the same effect than histamine  $4 \mu M$ , in spite of MCM contained a similar histamine concentration. Likely, this is due to the presence of ATP in the MCM, having a contrary effect to the histamine. MC-derived ATP seems to participate in microglia  $[Ca^{2+}]_i$  signaling, morphological changes and iba-1 expression but apparently, it does not influence the phagocytotic modifications mediated by the MCM. Large dense core granules of most of eukaryotic cells, accumulate ATP at large concentration ( $120-300 mM$ ) [33]. We do not know the concentration of ATP in the MCM used in our experiments but it is probable to be closer to  $100 \mu M$  than  $10 \mu M$ . Because certain dose dependence is observed on the response induced by ATP in microglial phagocytosis and Iba1 intensity (Fig. 5 and Fig. 6), it can be assumed that at higher rates of MC degranulation higher levels of ATP should be achieved and consequently, it would produce lower iba1 expression and a reduction in the phagocytosis rate induced by the MCM. Future research and determination of ATP levels in the MCM under different strength of MCs degranulation would help to better define how MCs are involved in the modulation of microglia functions.

Histamine has been previously probed to promote microglial phagocytosis via H1R [34] and the response was dose dependent (range from 1 to 100  $\mu\text{M}$ ). Here, we observed that histamine 4, 20 and 100  $\mu\text{M}$  have a similar rate of beads per cell. The H1 and H2 receptors have relatively low affinity for histamine (at the  $\mu\text{M}$  range) compared to their high affinity H3 and H4 counterparts (5–10 nM) [35]. Because of MCs release histamine at a concentration of the order of micromolar, even under basal conditions, presumably microglia in the surrounding of brain MC, should be activated. Although an inhibition of microglial phagocytosis was also reported through H3R at concentrations above 10  $\mu\text{M}$  of histamine [36], our results suggest microglial phagocytosis mediated by histamine and MCM depend on H1R activation exclusively.

Overall, our findings suggest that the microglia activation and the rise of internalized beads mediated by MCs in resting conditions (without degranulation) can be only elicited by histamine. However, an intensive degranulation of MCs should involve the release massive of mediators, such as ATP, that may induce an inhibition of the phagocytosis.

The role of MCs in determining the microglial phenotype in Alzheimer and other pathologies can be crucial [37, 38]. MCs are among the first brain cells to sense amyloid beta peptides [39] and MCs treated with  $\text{A}\beta$  enhanced histamine release [40] that, according to our data, could rise the microglial phagocytotic response. Features of microglia that relate to phagocytosis are beneficial in Alzheimer's disease by degrading  $\text{A}\beta$  plaques [41]. Therefore, the inhibition of MC degranulation could be a useful therapeutic strategy to limit brain histamine and ATP concentration and, as a result, reduce proinflammatory cytokines (TNF- $\alpha$ , IL-6) and modulate  $\text{A}\beta$  phagocytosis by microglia. Besides, a delicate regulation of the microglial phagocytosis seems to be critical in Parkinson disease, multiple sclerosis and other brain diseases [4, 42, 43].

We have recently demonstrated a bidirectional communication between MCs and hippocampal neurons [22]. Proteoglycans of CS released from MCs granules are involved in neuronal activation and  $[\text{Ca}^{2+}]_i$  elevation. While an acute stimulation of MCs can allow a rapid release of a small amount of histamine through kiss-and-run (reversible fusion), the intense and continuous MC activation would produce degranulation with massive histamine, ATP and proteoglycans extrusion [44] which can compromise microglial phagocytic clearance function and activate hippocampal neurons, and therefore contributing to increase neuronal  $[\text{Ca}^{2+}]_i$  overload and unwanted material among the CNS environment. Since the elimination of unwanted and potentially harmful matter is crucial for CNS function, regulation of microglia phagocytosis by MCs may have a key role in neuroinflammation.

## Conclusion

MCs-derived ATP and histamine are key molecules in the modulation of microglia phagocytosis which is crucial for CNS homeostasis. MCs are resident cells of the brain and one of the most important sources of histamine during systemic inflammation so that the control of degranulation by MCs stabilizers in combination with histamine and ATP receptors agonists/antagonists may be a valuable therapeutic approach in neuroinflammatory disorders.

## Abbreviations

MC (Mast cell); MCM (cocktail of MC mediators);  $[\text{Ca}^{2+}]_i$  (intracellular calcium concentration); PG (proteoglycans); CS (chondroitin sulfate); LPS (lipopolysaccharide); CNS (Central Nervous System).

## Acknowledgements

We thank Dolores Gutierrez and Laura Sánchez for their technical support. All data are available upon request.

### *Author Contributions*

J AFC, ASG, SBG, MDM and JA carried out all the experiments and data analysis. J AFC, PRP and EA designed experiments, analyzed and discussed results, and wrote the paper. All authors have read and approved the final manuscript.

### *Funding*

This work was supported by grants from FEDER/Ministerio de Ciencia, Innovación y Universidades – Agencia Estatal de Investigación/Proyecto (BFU2017-85832R) and the Junta de Andalucía (BIO-236).

### *Statement of Ethics*

The experiments carried out in this work have been approved by the Ethics Committees of Seville University School of Medicine and the Consejería de Agricultura, Pesca y Desarrollo Rural de la Junta de Andalucía, Spain.

## Disclosure Statement

The authors declare that they have no competing interests.

## References

- 1 Kovacs GG: Concepts and classification of neurodegenerative diseases. *Handb Clin Neurol* 2017;145:301-307.
- 2 Dugger BN, Dickson DW: Pathology of neurodegenerative diseases. *Cold Spring Harb Perspect Biol* 2017;9:a028035.
- 3 Kettenmann H, Hanisch UK, Noda M, Verkhratsky A: Physiology of microglia. *Physiol Rev* 2011;91:461-553.
- 4 Hanisch UK, Kettenmann H: Microglia: Active sensor and versatile effector cells in the normal and pathologic brain. *Nat Neurosci* 2007;10:1387-1394.
- 5 Sharma P, Ping L: Calcium ion influx in microglial cells: physiological and therapeutic significance. *J Neurosci Res* 2014;92:409-423.
- 6 Dou Y, Wu HJ, Li HQ, Qin S, Wang YE, Li J, et al.: Microglial migration mediated by ATP-induced ATP release from lysosomes. *Cell Res* 2012;22:1022-1033.
- 7 Imura Y, Morizawa Y, Komatsu R, Shibata K, Shinozaki Y, Kasai H, et al.: Microglia release ATP by exocytosis. *Glia* 2013;61:1320-1330.
- 8 Andrei C, Margiocco P, Poggi A, Lotti L V, Torrisi MR, Rubartelli A: Phospholipases C and A2 control lysosome-mediated IL-1 beta secretion: Implications for inflammatory processes. *Proc Natl Acad Sci U S A* 2004;101:9745-9750.
- 9 Eder C: Mechanisms of interleukin-1 $\beta$  release. *Immunobiology* 2009;214:543-553.
- 10 Greenberg S, el Khoury J, di Virgilio F, Kaplan EM, Silverstein SC: Ca(2+)-independent F-actin assembly and disassembly during Fc receptor-mediated phagocytosis in mouse macrophages. *J Cell Biol* 1991;113:757-767.
- 11 Kalla R, Bohatschek M, Kloss CUA, Krol J, Von Maltzan X, Raivich G: Loss of microglial ramification in microglia-astrocyte cocultures: involvement of adenylate cyclase, calcium, phosphatase, and Gi-protein systems. *Glia* 2003;41:50-63.
- 12 Silver R, Curley JP: Mast cells on the mind: new insights and opportunities. *Trends Neurosci* 2013;36:513-521.

- 13 Silverman AJ, Sutherland AK, Wilhelm M, Silver R: Mast cells migrate from blood to brain. *J Neurosci* 2000;20:401–408.
- 14 Wernersson S, Pejler G: Mast cell secretory granules: Armed for battle. *Nat Rev Immunol* 2014;14:478–494.
- 15 Galli SJ, Nakae S, Tsai M: Mast cells in the development of adaptive immune responses. *Nat Immunol* 2005;6:135–142.
- 16 Zhang S, Zeng X, Yang H, Hu G, He S: Mast cell tryptase induces microglia activation via protease-activated receptor 2 signaling. *Cell Physiol Biochem* 2012;29:931–940.
- 17 Zhang X, Wang Y, Dong H, Xu Y, Zhang S: Induction of Microglial Activation by Mediators Released from Mast Cells. *Cell Physiol Biochem* 2016;38:1520–1531.
- 18 Dong H, Zhang X, Wang Y, Zhou X, Qian Y, Zhang S: Suppression of Brain Mast Cells Degranulation Inhibits Microglial Activation and Central Nervous System Inflammation. *Mol Neurobiol* 2017;54:997–1007.
- 19 Dong H, Wang Y, Zhang X, Zhang X, Qian Y, Ding H, et al.: Stabilization of Brain Mast Cells Alleviates LPS-Induced Neuroinflammation by Inhibiting Microglia Activation. *Front Cell Neurosci* 2019;13:191.
- 20 Zhang X, Dong H, Li N, Zhang S, Sun J, Zhang S, et al.: Activated brain mast cells contribute to postoperative cognitive dysfunction by evoking microglia activation and neuronal apoptosis. *J Neuroinflammation* 2016;13:127.
- 21 Prada I, Furlan R, Matteoli M, Verderio C: Classical and unconventional pathways of vesicular release in microglia. *Glia* 2013;61:1003–1017.
- 22 Flores JA, Ramírez-Ponce MP, Montes MÁ, Balseiro-Gómez S, Acosta J, Álvarez de Toledo G, et al.: Proteoglycans involved in bidirectional communication between mast cells and hippocampal neurons. *J Neuroinflammation* 2019;16:107.
- 23 Parada E, Egea J, Buendia I, Negro P, Cunha AC, Cardoso S, et al.: The microglial  $\alpha 7$ -acetylcholine nicotinic receptor is a key element in promoting neuroprotection by inducing heme oxygenase-1 via nuclear factor erythroid-2-related factor 2. *Antioxid Redox Signal* 2013;19:1135–1148.
- 24 Lin L, Desai R, Wang X, Lo EH, Xing C: Characteristics of primary rat microglia isolated from mixed cultures using two different methods. *J Neuroinflammation* 2017;14:101.
- 25 Lian H, Roy E, Zheng H: Microglial Phagocytosis Assay. *Bio Protoc* 2016;6:e1988.
- 26 Davalos D, Grutzendler J, Yang G, Kim J V, Zuo Y, Jung S, et al.: ATP mediates rapid microglial response to local brain injury *in vivo*. *Nat Neurosci* 2005;8:752–758.
- 27 Liu GJ, Kalous A, Werry EL, Bennett MR: Purine release from spinal cord microglia after elevation of calcium by glutamate. *Mol Pharmacol* 2006;70:851–859.
- 28 Dong H, Zhang W, Zeng X, Hu G, Zhang H, He S, et al.: Histamine induces upregulated expression of histamine receptors and increases release of inflammatory mediators from microglia. *Mol Neurobiol* 2014;49:1487–500.
- 29 Imai Y, Kohsaka S: Intracellular Signaling in M-CSF-Induced Microglia Activation: Role of Iba1. *Glia* 2002;40:164–174.
- 30 Ito D, Tanaka K, Suzuki S, Dembo T, Fukuuchi Y: Enhanced expression of Iba1, ionized calcium-binding adapter molecule 1, after transient focal cerebral ischemia in rat brain. *Stroke* 2001;32:1208–1215.
- 31 Ito D, Imai Y, Ohsawa K, Nakajima K, Fukuuchi Y, Kohsaka S: Microglia-specific localisation of a novel calcium binding protein, Iba1. *Mol Brain Res* 1998;57:1–9.
- 32 Sasaki Y, Ohsawa K, Kanazawa H, Kohsaka S, Imai Y: Iba1 is an actin-cross-linking protein in macrophages/microglia. *Biochem Biophys Res Commun* 2001;286:292–297.
- 33 Mark Wightman R, Domínguez N, Borges R: How intravesicular composition affects exocytosis. *Pflugers* 2018;470:135–141.
- 34 Rocha SM, Saraiva T, Cristóvão AC, Ferreira R, Santos T, Esteves M, et al.: Histamine induces microglia activation and dopaminergic neuronal toxicity via H1 receptor activation. *J Neuroinflammation* 2016;13:137.
- 35 Alexander SPH, Christopoulos A, Davenport AP, Kelly E, Mathie A, Peters JA, et al.: THE CONCISE GUIDE TO PHARMACOLOGY 2019/20: G protein-coupled receptors. *Br J Pharmacol* 2019;176:S21–141.
- 36 Iida T, Yoshikawa T, Matsuzawa T, Naganuma F, Nakamura T, Miura Y, et al.: Histamine H3 receptor in primary mouse microglia inhibits chemotaxis, phagocytosis, and cytokine secretion. *Glia* 2015;63:1213–1225.

- 37 Kempuraj D, Selvakumar GP, Thangavel R, Ahmed ME, Zaheer S, Raikwar SP, et al.: Mast Cell Activation in Brain Injury, Stress, and Post-traumatic Stress Disorder and Alzheimer's Disease Pathogenesis. *Front Neurosci* 2017;11:703.
- 38 Hendriksen E, van Bergeijk D, Oosting RS, Redegeld FA: Mast cells in neuroinflammation and brain disorders. *Neurosci Biobehav Rev* 2017;79:119–133.
- 39 Niederhoffer N, Levy R, Sick E, Andre P, Coupin G, Lombard Y, et al.: Amyloid  $\beta$  Peptides Trigger CD47-Dependent Mast Cell Secretory and Phagocytic Responses. *Int J Immunopathol Pharmacol* 2009;22:473–483.
- 40 Harcha PA, Vargas A, Yi C, Koulakoff AA, Giaume C, Sáez JC: Hemichannels are required for amyloid  $\beta$ -Peptide-induced degranulation and are activated in brain mast cells of APPswe/PS1dE9 Mice. *J Neurosci* 2015;35:9526–9538.
- 41 Majumdar A, Cruz D, Asamoah N, Buxbaum A, Sohar I, Lobel P, et al.: Activation of microglia acidifies lysosomes and leads to degradation of Alzheimer amyloid fibrils. *Mol Biol Cell* 2007;18:1490–1496.
- 42 Fu R, Shen Q, Xu P, Luo JJ, Tang Y: Phagocytosis of microglia in the central nervous system diseases. *Mol Neurobiol* 2014;49:1422–1434.
- 43 Tremblay M-E, Cookson MR, Civiero L: Glial phagocytic clearance in Parkinson's disease. *Mol Neurodegener* 2019;14:16.
- 44 Flores JA, Balseiro-Gómez S, Ales E: Emerging Roles of Granule Recycling in Mast Cell Plasticity and Homeostasis. *Crit Rev Immunol* 2016;36:461–484.